# Comparison of semiclassical, quasiclassical, and exact quantum transition probabilities for the collinear $H + H_2$ exchange reaction*

Joel M. Bowman† and Aron Kuppermann

*A. A. Noyes Laboratory of Chemical Physics,‡ California Institute of Technology, Pasadena, California 91109*

(Received 13 August 1973)

Using the classical (CSC), primitive (PSC), and uniform (USC) semiclassical expressions for transition probabilities given by Miller and co-workers, we have calculated the reactive and nonreactive $0 \rightarrow 0$ and $0 \rightarrow 1$ transition probabilities for the collinear $H + H_2$ exchange reaction. Comparison with previously calculated exact quantum and quasiclassical results for the reactive and nonreactive $0 \rightarrow 0$ transitions reveals that the semiclassical approximations are not very good, especially the CSC and PSC ones. All three semiclassical probabilities for the reactive $0 \rightarrow 0$ transition exceed unity in the collision energy range from 0.0 to 0.2 eV above the quasiclassical reaction threshold. This feature coupled with the failure of any of the semiclassical approximations to produce the marked quantum effects present in this transition causes these results to be less accurate than the corresponding quasiclassical ones. For the reactive and nonreactive $0 \rightarrow 1$ transitions the USC results are in qualitative agreement with the exact quantum ones and are better than the standard quasiclassical results. However, the reverse quasiclassical results are almost as good as the USC ones for these transitions. A probable reason for the inability of the USC expression to produce the strong oscillations observed in the exact quantum results is that the latter are due to interference between direct and resonant (i.e., compound state) processes whereas the present formulation of the semiclassical method does not encompass such phenomena. A comparison of the total reaction probabilities obtained by the USC and quasiclassical methods with the exact quantum one indicates that the USC result is more accurate than the quasiclassical one, except at collision energies less than 0.50 eV. This improved accuracy is due to a partial cancellation of errors in the contributing $0 \rightarrow 0$ and $0 \rightarrow 1$ USC reactive transition probabilities.

## I. INTRODUCTION

There has recently been much progress in the development of a semiclassical theory of reactive and nonreactive atom–molecule scattering.[1-6] The central theme of this theory is derived from the superposition principle of quantum mechanics. One assumes that "quantum effects" in heavy particle (e.g., atom-molecule) systems are due primarily, if not solely, to the interference of scattering amplitudes. It has been shown that the classical limit of the scattering matrix is obtained from information contained in the exact classical trajectories describing the atom–molecule scattering. The phases of the S matrix elements are given by the action accrued along trajectories whose boundary conditions correctly describe the scattering process of interest and the absolute values of those elements are obtainable from the phases.[1a]

In a numerical application of his theory, Miller[1b] computed the transition probabilities for the translational to vibrational energy transfer in collinear collisions of an atom (He) with a harmonic oscillator ($H_2$). He found, typically, two classical trajectories satisfying the correct boundary conditions. This feature gave rise to "uniform" (USC) and "primitive" (PSC) semiclassical expressions for the transition probabilities. A "classical" (CSC) semiclassical expression also resulted by ignoring the interference term in the primitive semiclassical expressions. The agreement between the CSC and PSC results and the exact quantum ones of Secrest and Johnson[7] was not very good. However, the USC results gave excellent agreement. Furthermore, a "rainbow" phenomenon caused the CSC and PSC results to diverge at certain energies, whereas the corresponding USC results were well-behaved. Rankin and Miller[1e] studied the collinear $H + Cl_2 \rightarrow HCl + Cl$ reaction semiclassically. They found that the final quantum number of the product molecule was an anomalously random function of the initial phase angle of the reagent molecule, and this precluded the use of the USC, PSC, and CSC expressions. Miller and co-workers[1f,1g,1h] have treated the collinear and three-dimensional $H + H_2$ exchange reaction at collision energies below the quasiclassical reaction threshold by employing complex-valued classical trajectories. They compared their collinear results with two different "exact" quantum calculations.[8,9] In one[8] a Porter–Karplus[10] potential energy surface was used, whereas in the other[9] a harmonic-type approximation to this surface was employed. These exact quantum calculations differed from one another by a factor of two or more over the energy range of interest and therefore the most appropriate comparison is with the former calculation.[11]

No extensive comparison between semiclassical, exact quantum and quasiclassical transition probabilities for a chemical reaction has yet been made. In this paper we present such a comparison for the reactive and nonreactive transition probabilities for the collinear H + $H_2$ exchange reaction. The quantum results we compare with are those of Truhler and Kuppermann[12] and Schatz and Kuppermann[13] and the quasiclassical ones are those of Bowman and Kuppermann.[14] The potential energy surface used in all these calculations was a Wall–Porter fit[15] to a scaled SSMK surface[16] and is described in detail elsewhere.[12] The range of total energies considered, 0 to 1.30 eV, includes energies for which vibrationally excited reagent and/or product $H_2$ are present. Some of the results of the present paper were presented in a preliminary form previously.[17]

## II. CALCULATIONAL PROCEDURES

### A. Semiclassical Expressions

The theoretical basis for the semiclassical method is described in detail elsewhere.[1a,1b,1e,6] We summarize here the procedure followed in our calculations.

Let us consider the collinear A + BC → AB + C reaction. We define $R^{\alpha(\beta)}$ to be the distance from the atom to the center of mass of the diatom in arrangement channel $\alpha(\beta)$, where $\alpha, \beta = 1, 2$. Arrangement channels 1 and 2 are A + BC and AB + C, respectively. AC + B is excluded by the collinear nature of the reaction. The break-up arrangement A + B + C is also excluded. The relative momentum variable conjugate to $R^{\alpha(\beta)}$ is $P_R^{\alpha(\beta)}$. The internal diatom angle variable is $q^{\alpha(\beta)}$ and its conjugate momentum is $M^{\alpha(\beta)}$. The diatom internuclear distance coordinate and momentum are respectively $r^{\alpha(\beta)}$ and $P_r^{\alpha(\beta)}$. Consider a reactive or nonreactive transition from the reagent state $M^\alpha = n^\alpha$ to the product state $M^\beta = m^\beta$, where $n^\alpha$ and $m^\beta$ are given integers. To investigate this transition semiclassically at a given total energy $E$ a search of classical trajectories is carried out as follows. At time $t_0$ the initial atom–molecule separation is fixed at some large value, $R_0^\alpha$, such that the interaction energy is negligibly small. $P_R^\alpha$ is obtained from the relative collision energy $E_{n\alpha}^\alpha$ through the usual expression

$$P_{R_0}^\alpha = -[2\mu_\alpha E_{n\alpha}^\alpha]^{1/2} \quad ,$$

where $\mu_\alpha$ is the reduced mass of the atom–diatom system in the $\alpha$ arrangement channel. $E$ is equal to $E_{n\alpha}^\alpha + E(n^\alpha)$, where $E(n^\alpha)$ is the semiclassical diatom energy eigenvalue. The initial value of the angle variable $q_0^\alpha$ is made to scan uniformly the range 0 to $2\pi$ and the corresponding initial value $r_0^\alpha$ of $r^\alpha$ is obtained from the relationship[18a]

$$\partial F_2(n^\alpha, r_0^\alpha)/\partial n^\alpha = q_0^\alpha \quad .$$

For a Morse oscillator an exact analytical expression for the function $r_0^\alpha = r_0^\alpha(q_0^\alpha)$ is available[1e] and was used in our calculations. $F_2(n^\alpha, r^\alpha)$ is the classical generating function which is the solution to the time-independent Hamilton–Jacobi Equation.[18b] The initial momentum $P_{r_0}^\alpha$ can be obtained from $n^\alpha$, $q_0^\alpha$, and $r_0^\alpha$ using the expression[18a]

$$\partial F_2(n^\alpha, r^\alpha)/\partial r_0^\alpha = P_{r_0}^\alpha \quad ,$$

from which one obtains

$$P_{r_0}^\alpha = \mathrm{sign}(\pi - q_0^\alpha)\{2\mu^\alpha[E(n^\alpha) - V^\alpha(r_0^\alpha)]\}^{1/2} \quad ,$$

where $\mu^\alpha$ is the reduced mass of the diatom and $V^\alpha$ is its internal potential energy function. The quantities $R_0^\alpha$, $P_{R_0}^\alpha$, $r_0^\alpha$, and $P_{r_0}^\alpha$ thus chosen furnish the initial conditions needed to integrate Hamilton's equations of motion. This integration is performed and the variables $R^{\beta(\alpha)}$, $P_R^{\beta(\alpha)}$, $r^{\beta(\alpha)}$ and $P_r^{\beta(\alpha)}$ are obtained as a function of time. At time $t_1$, when $R_R^{\beta(\alpha)}$ is equal to some large value $R_1^{\beta(\alpha)}$, the quantity $M^\beta = M^\beta(q_0^\alpha; n^\alpha, E)$ is calculated (for fixed values of $n^\alpha$ and $E$) and root(s) to the equation

$$M^\beta(q_0^\alpha; n^\alpha, E) = m^\beta \tag{1}$$

are sought for. Several possible outcomes exist.

The usual outcome is that there are two isolated, though perhaps coalescent, roots to Eq. (1). The uniform semiclassical (USC) expression for the reaction probability to form product AB in the $m$th vibrational state from reagent BC in the $n$th vibrational state is given by[1b,1e,2b,6]

$$P_{m\beta n\alpha}^{\mathrm{USC}} = [p_1^{1/2} + p_2^{1/2}]^2 \pi z^{1/2} A_i^2(-z) + (p_1^{1/2} - p_2^{1/2})^2 \times \pi z^{1/2} B_i^2(-z) \quad , \tag{2}$$

where

$$p_j = (2\pi\hbar|\,\partial M^\beta(q_0^\alpha; n^\alpha, E)/\partial q_0^\alpha\,|_{q_{0_j}^\alpha})^{-1} \quad , \quad j = 1, 2$$

and

$$z = [\tfrac{3}{4}|\,\Delta_1 - \Delta_2\,|]^{2/3} \quad .$$

The subscript $j$ labels the two values of $q_0^\alpha$ which give rise to the two trajectories such that $M^\beta = m^\beta$. The $\Delta_j$ are calculated from the corresponding trajectories by[1e,6]

$$\Delta_j = \hbar^{-1}\{\int_{t_0}^{t_1} dt\,[P_R^\alpha(t)\,dR^\alpha(t) + P_r^\alpha(t)\,dr^\alpha(t)] \times (\text{calculated along the } j\text{th trajectory}) + F_2(r_j^\alpha(t_0), n^\alpha) + P_R^\alpha(t_0)\,R^\alpha(t_0) - F_2(r_j^\beta(t_1), m^\beta) - P_R^\beta(t_1)\,R^\beta(t_1)\} \quad . \tag{3}$$

$A_i(-z)$ and $B_i(-z)$ are respectively the regular and irregular Airy functions.[19] This $\Delta_j$ given by Eq. (3) is a discontinuous function of $q_0^\alpha$ since the function sign $[P_r^\alpha(r_0^\alpha(q_0^\alpha))]$ contained in the $F_2$ gen-

erating function is a discontinuous function. The spurious discontinuities introduced by this feature can be eliminated in several ways. The one we adopted is to modify $\Delta_j$ as follows[6]:

$$\Delta_j = \hbar^{-1}\{\int_{t_0}^{t_1} dt\,[P_R^\alpha(t)\,dR^\alpha(t) + P_r^\alpha(t)\,dr^\alpha(t)] + P_R^\alpha(t_0)\,R^\alpha(t_0) - P_R^\beta(t_1)\,R^\beta(t_1) + F_2(r^\alpha(t_0), n^\alpha) - [\mathrm{sign}(P_r^\alpha(r_0^\alpha)) - 1](n^\alpha + \tfrac{1}{2})\,\pi\hbar - F_2(r^\beta(t_1), m^\beta) + [\mathrm{sign}(P_r^\beta(r_1^\beta) - 1)](m^\beta + \tfrac{1}{2})\,\pi\hbar\} \quad . \tag{4}$$

In the limit of $|\Delta_1 - \Delta_2| \gg 1$, Eq. (2) becomes asymptotically equal to the primitive semiclassical (PSC) expression given by

$$P_{m\beta n\alpha}^{\mathrm{PSC}} = p_1 + p_2 + 2(p_1 p_2)^{1/2}\sin(\Delta_1 - \Delta_2) \quad . \tag{5}$$

By omitting the "interference" term $2(p_1 p_2)^{1/2} \times \sin(\Delta_1 - \Delta_2)$ in Eq. (5) the classical semiclassical (CSC) expression results, viz.,

$$P_{m\beta n\alpha}^{\mathrm{CSC}} = p_1 + p_2 \quad . \tag{6}$$

In another case, only one trajectory may yield a root to Eq. (1). As a consequence the USC, PSC, and CSC expressions all become equal to

$$P_{m\beta n\alpha}^{\mathrm{SC}} = p_1 \quad . \tag{7}$$

A third possibility is that no (real-valued) classical trajectory yields the desired root. In this case, in the absence of analytical continuation techniques[1b,1c,2b] or the inclusion of complex-valued trajectories[1f,1g,1h,2f] it is found that

$$P_{m\beta n\alpha}^{\mathrm{SC}} \equiv 0 \quad .$$

In the calculations we report in Sec. III, no attempt to analytically continue by power series techniques or by employing complex-valued trajectories was made.

A fourth and very rare case is one in which a continuous range of values $q_{0l}^\alpha$ to $q_{0u}^\alpha$ yields roots to Eq. (1). In this case we have shown that the semiclassical **S** matrix element is given by[6]

$$S_{m\beta n\alpha}^{\mathrm{SC}} = \int_{q_{0l}^\alpha}^{q_{0u}^\alpha} dq_0^\alpha\,\psi_{m\beta}^{*sc}(r_1^\beta)(2\pi i\hbar)^{-1/2}[\partial r_1^\beta/\partial q_0^\alpha]^{1/2} \times \exp[i\delta/\hbar] \quad , \tag{8}$$

where

$$\delta = \int_{t_0}^{t_1} dt\left[P_R^\alpha(t)\frac{dR^\alpha(t)}{dt} + P_r^\alpha(t)\frac{dr^\alpha(t)}{dt}\right] + F_2(r_0^\alpha(q_0^\alpha), n^\alpha) + P_R^\alpha(t_0)\,R^\alpha(t_0) - P_R^\beta(t_1)\,R^\beta(t_1) \quad .$$

$\psi_{m\beta}^{sc}(r_1^\beta)$ is the JWKB wavefunction for the diatom in arrangement channel $\beta$. The reaction probability is then

$$P_{m\beta n\alpha}^{\mathrm{SC}} = |S_{m\beta n\alpha}^{\mathrm{SC}}|^2 \quad .$$

No calculations of reaction probabilities based on Eq. (8) are reported in the present paper, although we shall see a situation where it approximately applies.

In reporting our results of calculations we adopt the following convention:

$$P_{nm}^R \equiv P_{m\beta n\alpha} \quad \alpha \neq \beta$$

$$P_{nm}^V \equiv P_{m\beta n\alpha} \quad \alpha = \beta \quad .$$

### B. Numerical Methods

CSC, PSC, and USC $P_{00}^R$, $P_{00}^V$, $P_{01}^R$, and $P_{01}^V$ transition probabilities were calculated as a function of energy for the collinear $H + H_2 \rightarrow H_2 + H$ reaction using the same potential energy surface employed in the exact quantum and quasiclassical calculations.[12,13,14]

The classical trajectories needed for the semiclassical calculations described in Sec. II.A were computed as follows. An initial atom–molecule separation $R_0$ of 4.6 bohr was chosen, for which the corresponding interaction energy vanishes. Typically 100 values of $q_0$ uniformly spaced in the interval 0 to $2\pi$ were chosen, thereby generating 100 trajectories per energy. The integration of Hamilton's equations was performed using a fourth order Runge–Kutta–Gill initiator and an Adams–Moulton fourth order predictor, fifth order corrector.[20] The associated action $\Delta_j$ [see Eq. (4)] was checked by testing its invariance with respect to the initial and final integration times $t_0$ and $t_1$. The same results to within a few parts in $10^4$ were obtained using either the reagent or product coordinate system. This, coupled with the general result that action differences $|\Delta_1 - \Delta_2|$ for two trajectories were generally less than unity resulted in transition probabilities precise to $\pm 0.01$. Computational time for one trajectory and its associated action in double precision arithmetic was 3 to 4 seconds on an IBM 370/155.

### C. Behavior of Action Difference as a Function of Initial Phase

In order to illustrate the differences between $\Delta$ given by Eq. (4) and $\Delta$ given by Eq. (3) we have plotted these two $\Delta$'s as a function of $q_0$ for a total energy $E$ of 1.053 eV in Fig. 1. There, and more quantitatively in Table I, the continuity of $\Delta$ given by Eq. (4) and the discontinuous behavior of $\Delta$ given by Eq. (3) is demonstrated. We always used Eq. (4) to calculate $\Delta$.

## III. RESULTS

### A. General Features of the Semiclassical Transition Probabilities

As discussed in Sec. II the location of root(s) to Eq. (1) of Sec. II.A necessary in order to compute the CSC, PSC, and USC transition probabilities requires a scan of the final action number $m$ of the product versus the initial angle variable $q_0$ of the

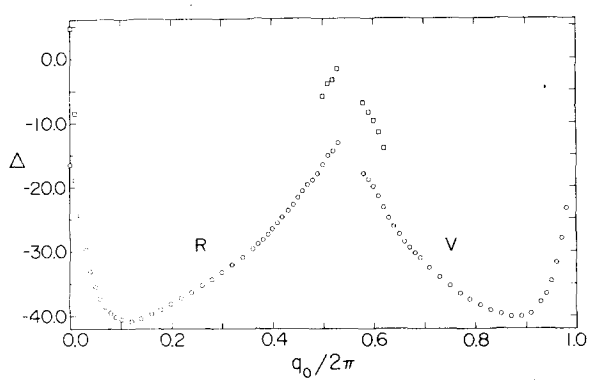


FIG. 1. Corrected [circles; Eq. (4)] and uncorrected [squares; Eq. (3)] action Δ as a function of the initial phase angle $q_0$ for reactive ($R$) and nonreactive ($V$) trajectories. The total energy is 1.053 eV. For initial phases for which only circles are indicated, Eqs. (4) and (3) furnish the same value of Δ.

TABLE I. Action difference Δ and final action number $m$ versus initial phase angle $q_0$ in vicinity of discontinuities.[a]

| $q_0$ | Type of collision | $m$ | $\Delta^{b,c}$ | $\Delta^{b,d}$ |
|---|---|---|---|---|
| 0.07359 | Reactive | 1.057 | −10.88 | −20.66 |
| 0.07372 | Reactive | 1.056 | −20.68 | −20.68 |
| 3.15995 | Reactive | 1.141 | −17.52 | −17.52 |
| 3.16300 | Reactive | 1.142 | −7.17 | −17.49 |
| 4.01125 | Nonreactive | 0.9012 | −15.75 | −24.56 |
| 4.01251 | Nonreactive | 0.8994 | −24.58 | −24.58 |
| 6.21810 | Nonreactive | 1.021 | −21.26 | −21.26 |
| 6.23562 | Nonreactive | 1.022 | −11.69 | −21.25 |

[a]The total energy $E$ is 1.053 eV.
[b]The action difference Δ is in units of $\hbar$.
[c]Δ given by Eq. (3).
[d]Δ given by Eq. (4).

reagent. (For simplicity in presentation we have omitted the superscripts on the variables $m$ and $q_0$ and will use lower case $m$ in place of upper case $M$.) A typical result of such a scan is shown in Fig. 2 for trajectories computed at a total energy $E$ of 1.253 eV and for the reagent in its ground vibrational state. Several important features may be noted. Firstly, the reactive branch (solid curve) and the nonreactive branch (dashed curve) each have two roots to the equation $m=1$, i.e., two trajectories leading to a final $H_2$ with internal energy $E(1)$. Secondly, we note that there are no reactive trajectories for which $m=0$ in spite of the fact that this state is energetically accessible. In this case the semiclassical CSC, PSC, and USC reaction probabilities are set equal to zero, as stated in Sec. II, and the corresponding transition is usually termed "classically forbidden"[1b,2a] at this particular energy. The nonreactive transition $0\rightarrow 0$ is "allowed," however, since there are two trajectories corresponding to it. Another feature of interest is the fact that these curves almost reach the value $m=2$. The reactive and non-reactive transition $0\rightarrow 2$ are strictly forbidden for lack of sufficient energy. Thus, we prefer to term the $0\rightarrow 0$ reactive transition *dynamically inaccessible* and the transition $0\rightarrow f(f\geq 2)$ *energetically inaccessible* to stress the fact that the corresponding transition probabilities vanish for different reasons.

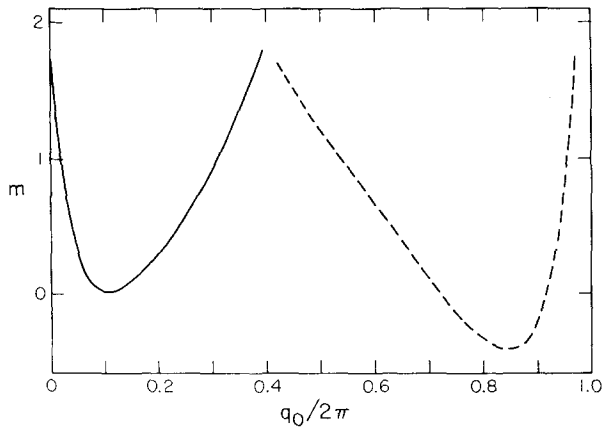


FIG. 2. Reactive (solid curve) and nonreactive (dashed curve) final action number, $m$, as a function of initial phase angle, $q_0$. The total energy is 1.253 eV.

### B. Comparison of Semiclassical, Quantum, and Quasiclassical Transition Probabilities

For the quasiclassical trajectories we define the vibrational quantum number of the final $H_2$ molecule as follows.[21] Let $\Delta E(n)=E(n+1)-E(n)$ and $E^v_{Cl}$ be the continuous classical vibrational energy of that molecule. If $E(n)\leq E^v_{Cl}<E(n)+\frac{1}{2}\Delta E(n)$ or $E(n)+\frac{1}{2}\Delta E(n)\leq E^v_{Cl}<E(n+1)$ we set $v=n$ or $v=n+1$, respectively. If $E^v_{Cl}\leq E(0)$, we set $v=0$. The quasiclassical transition probability to state $v$ is then defined as the fraction of the trajectories leading to $H_2$ in that state.

Figure 3 shows the USC, exact quantum, and quasiclassical $P^R_{00}$ transition probabilities as a function of the total energy $E$ and the initial translational energy $E_0$. The arrows on the lower abscissa designate the total energies at which excited vibrational states $v=1, 2$ become energetically accessible. The quasiclassical results have been compared to the exact quantum ones in some detail elsewhere.[14] The USC values are a better approximation at total energies greater than 1.0 eV, but deviate rapidly from the exact quantum ones as the energy decreases below 0.85 eV. Further,

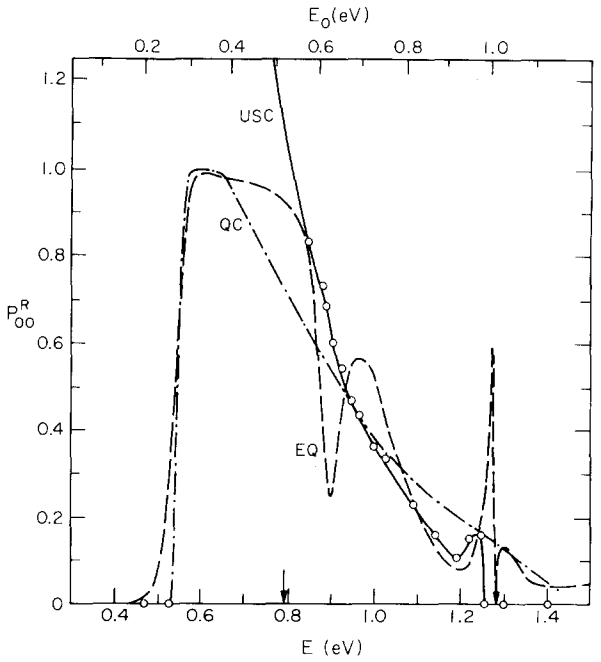


FIG. 3. Uniform semiclassical (solid curve), exact quantum (dashed curve), and quasiclassical (dashed–dotted curve) $P_{00}^R$ transition probabilities as a function of total energy, $E$, and initial translational energy, $E_0$.

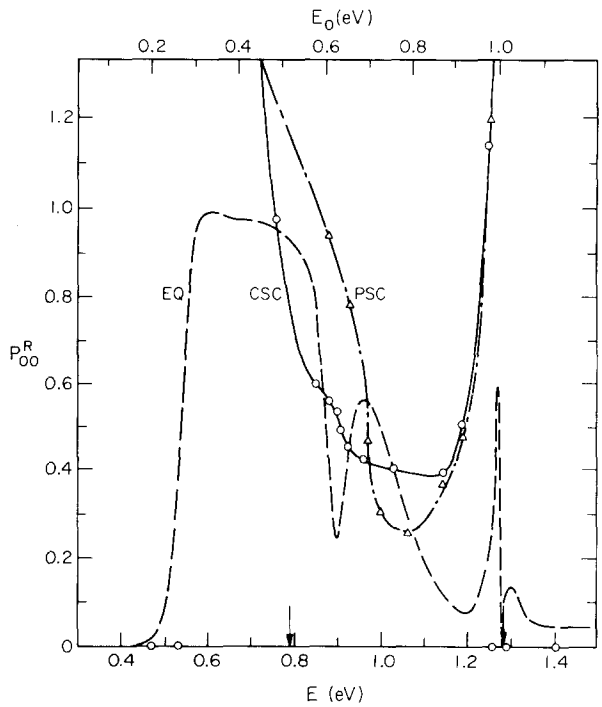


FIG. 5. Classical semiclassical (solid curve), primitive semiclassical (dashed-dotted curve), and exact quantum (dashed curve) $P_{00}^R$ transition probabilities as a function of total energy, $E$, and initial translational energy, $E_0$.

the strong oscillation occurring around $E = 0.95$ eV in the exact quantum curve is barely perceptible in the USC one. In addition, the dramatically sharp behavior in the quantum reaction probability at $E = 1.27$ eV is not produced by the USC result. (This quantum effect was not present in the quantum results used in our preliminary comparison.[17]) No USC results are given for total energies less than 0.78 eV because the $m$ versus $q_0$ curve was nearly horizontal at these lower energies and hence preclude the use of the USC, as well as the CSC and PSC expressions. This feature is illustrated in Fig. 4 where a plot of the final action number $m$ versus initial phase angle $q_0$ is shown for $E = 0.553$ eV. $m$ is seen to deviate only slightly from zero for both the reactive and non-reactive curves. Thus, practically every trajectory yields a root for the $0 \rightarrow 0$ transition and hence contributions about equally to the corresponding transition probability. As a result, the assumptions which lead to the USC, PSC, and CSC expressions[1b,6] are violated and these expressions cannot be used. The behavior of $m(q_0)$ shown in Fig. 4 is approximately like the one for which the integral representation of the $S$ matrix given by Eq. (8) of Sec. II is valid. Hence, this may be the only valid expression of usefulness. By contrast, at this energy the quasiclassical results is in good agreement with the exact quantum result. In Fig. 5 we give the CSC and PSC results for the $P_{00}^R$ transition probability along with the exact quantum ones. We note a divergent behavior in the CSC and PSC results at total energies around 1.25 eV. This behavior is easily understood by inspection of Fig. 2 from which it can be surmised that at an energy slightly less than 1.253 eV the reactive $m$ versus $q_0$ curve is tangent to the line $m = 0$ and hence $|\partial q_0/\partial m|_{m=0} \rightarrow \infty$. This fact causes the PSC and CSC results to diverge. The USC result, however, is well-behaved and in fact is in reasonable agree-

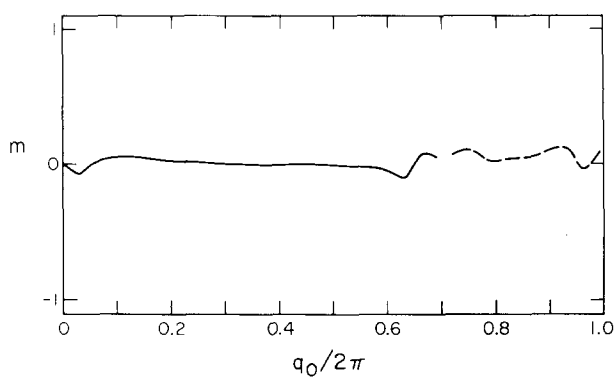


FIG. 4. Reactive (solid curve) and nonreactive (dashed-curve) final action number, $m$, as a function of initial phase angle, $q_0$. The total energy is 0.558 eV.

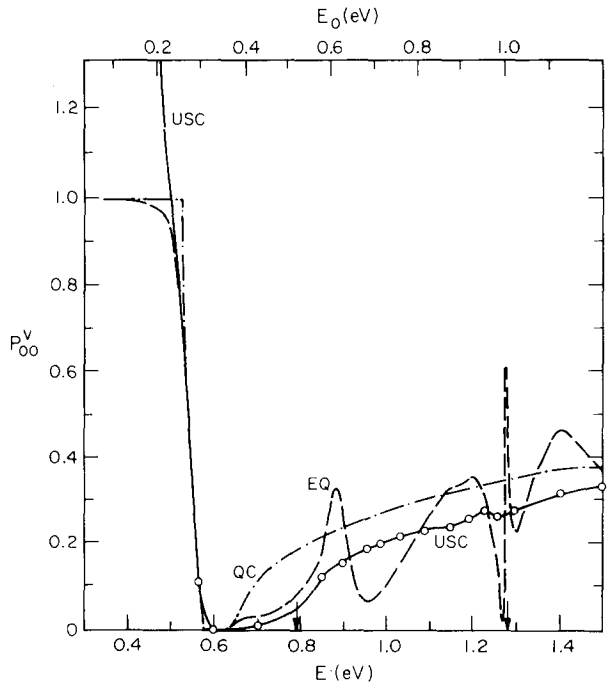


FIG. 6. Uniform semiclassical (solid curve), exact quantum (dashed curve), and quasiclassical (dashed–dotted curve) $P_{00}^{V}$ transition probabilities as a function of total energy, $E$, and initial translational energy, $E_0$.

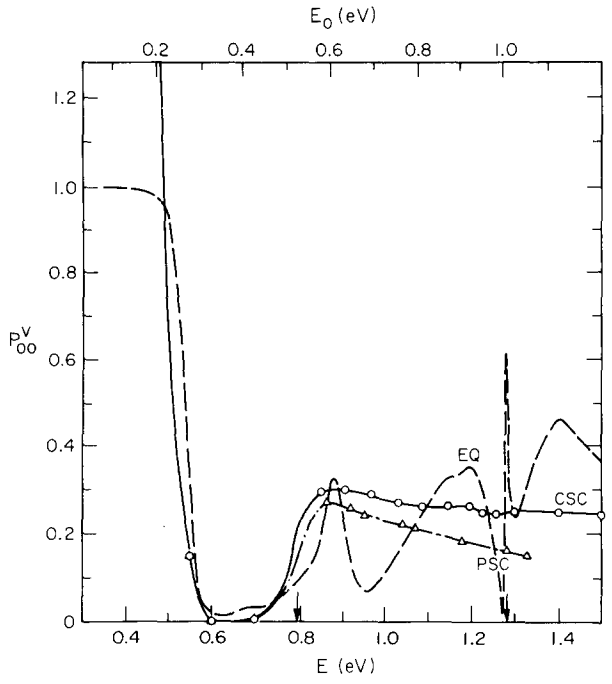


FIG. 7. Classical semiclassical (solid curve), primitive semiclassical (dashed–dotted curve) and exact quantum (dashed curve) $P_{00}^{V}$ transition probabilities as a function of total energy, $E$, and initial translational energy, $E_0$.

ment with the exact quantum result. This rainbow phenomenon has been observed and discussed by Miller.[1b]

In Figs. 6 and 7 we give the USC, exact quantum, quasiclassical and CSC, PSC, and exact quantum $P_{00}^{V}$ transition probabilities, respectively. The highly oscillatory nature of the quantum curve is not reproduced by the USC curve which in addition deviates from it rapidly as the energy decreases below 0.58 eV. The USC results do, however, show an increase with energy for $E > 0.85$ eV in agreement with the average trend of the exact results. This behavior is also exhibited by the quasiclassical results which in addition are well-behaved at low energies. The CSC and PSC curves are even worse approximations to the exact result than the USC one.

The USC, exact quantum, and quasiclassical $P_{01}^{R}$ transition probabilities are plotted in Fig. 8. The overall structure of the quantum curve is qualitatively reproduced by the USC one but not by the quasiclassical one. A difference of approximately 0.08 eV (1.9 kcal/mole) in the effective threshold energies of the quantum and USC results can be seen. The quasiclassical curve exhibits an unreasonable threshold behavior, i.e., nonzero, $P_{01}^{R}$ at total energies less than $E(1)$ (0.7945 eV). This results from the definition of the quasiclassical transition probability we have used, for which the energy at which $v = 1$ becomes accessible is $E(1) - \frac{1}{2}[E(1) - E(0)]$. This unreasonable threshold behavior of the quasiclassical $P_{01}^{R}$ transition probability can be removed by introducing the quasi-

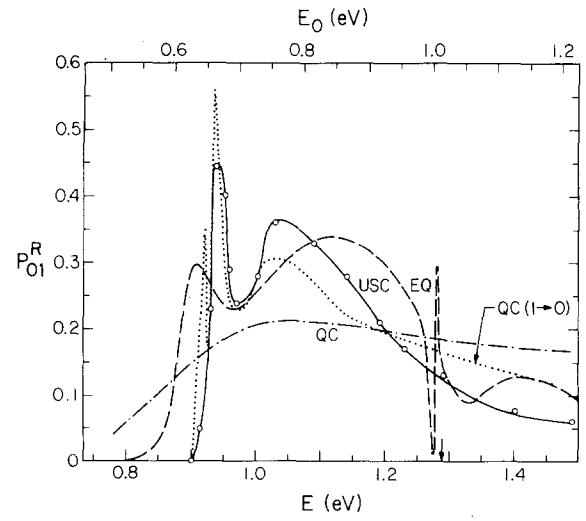


FIG. 8. Uniform semiclassical (solid curve), exact quantum (dashed curve), quasiclassical (dashed–dotted curve) $P_{01}^{R}$ transition probabilities and quasiclassical (dotted curve), $P_{10}^{R}$ transition probability as a function of total energy $E$ and initial translational energy $E_0$.

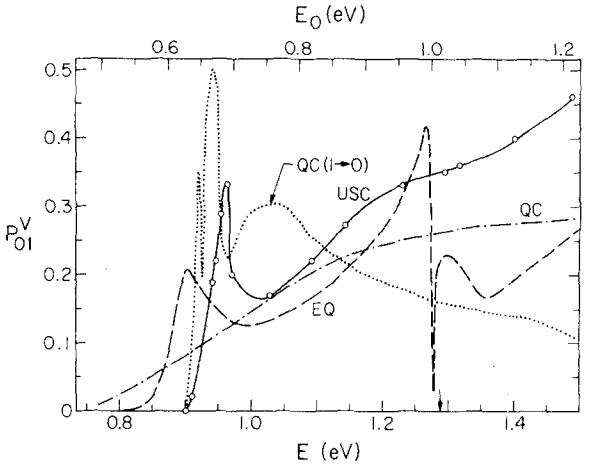


FIG. 9. Uniform semiclassical (solid curve), exact quantum (dashed curve), and quasiclassical (dashed–dotted curve) $P_{01}^{V}$ transition probabilities as a function of total energy $E$ and initial translational energy $E_0$.

classical $P_{10}^{R}$ transition probability which we can consider as the reverse $P_{01}^{R}$ transition probability. Since the quasiclassical $P_{01}^{R}$ and $P_{10}^{R}$ transition probabilities are not equal, whereas the semiclassical and exact quantum ones are (see next section) we have investigated the quasiclassical $P_{10}^{R}$ transition probability also. As seen in Fig. 8 this transition probability gives results in substantially better agreement with the exact $P_{01}^{R}$ ones than the quasiclassical $P_{01}^{R}$ transition probability. Indeed, the $P_{10}^{R}$ quasiclassical results are only slightly worse than the USC $P_{01}^{R}$ ones.

Figure 9 shows the USC, exact quantum, and quasiclassical $P_{01}^{V}$ transition probabilities. Here again, substantial qualitative agreement is found between the USC and the quantum results. As expected, the quasiclassical curve shows the correct average behavior but none of the structure of the quantum one, and shows improper threshold behavior. A difference in threshold energies of approximately 0.08 eV is again observed between the USC and exact results. We have also plotted the reverse $P_{01}^{V}$ (i.e., the $P_{10}^{V}$ transition probability) transition probability and note that although the threshold behavior of the $P_{10}^{V}$ result is more reasonable than the $P_{01}^{V}$ result with respect to proper threshold behavior, its spikey behavior is grossly incorrect.

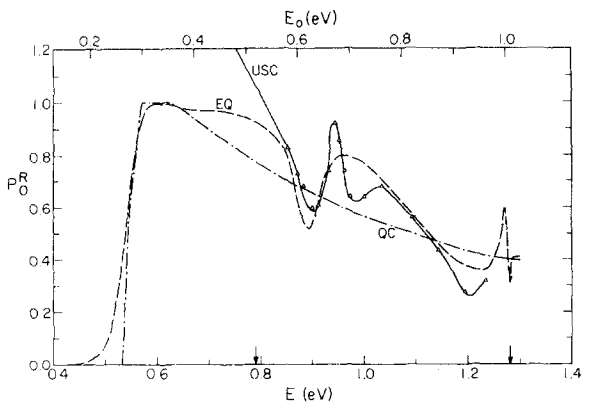


FIG. 10. Uniform semiclassical (solid curve), exact quantum (dashed curve), and quasiclassical (dashed–dotted curve) total reaction probability $P_0^R$ as a function of total energy $E$ and initial translational energy $E_0$.

TABLE II. Microscopic reversibility of semiclassical transition probabilities.

| | $E=0.953$ eV | $E=1.033$ eV |
|---|---|---|
| $P_{01}^{R}$ (USC) | 0.40 | 0.37 |
| $P_{10}^{R}$ (USC) | 0.41 | 0.37 |
| $P_{01}^{R}$ (quasiclassical) | 0.18 | 0.21 |
| $P_{10}^{R}$ (quasiclassical) | 0.38 | 0.45 |
| $P_{01}^{V}$ (USC) | 0.30 | 0.19 |
| $P_{10}^{V}$ (USC) | 0.31 | 0.18 |
| $P_{01}^{V}$ (quasiclassical) | 0.10 | 0.17 |
| $P_{10}^{V}$ (quasiclassical) | 0.08 | 0.07 |

The total reaction probability $P_0^R$ which is simply the sum $\sum_f P_{0f}^{R}$ is displayed in Fig. 10 where we compare the USC, the quasiclassical, and the exact quantum results. While the quasiclassical curve looks much like an averaged quantum one, the USC curve bears some resemblance to the exact one for total energies exceeding the $v=1$ threshold. This latter behavior is surprising since the strong oscillation present in the exact $P_{00}^{R}$ transition probability at energies slightly above the $v=1$ threshold is not apparent in the corresponding USC one. Nevertheless the oscillation in the exact quantum total reaction probability at energies around 0.90 eV appears in the USC result even though not in the quasiclassical one. This seems to be due to a fortuitous cancellation of errors in the uniform $0\rightarrow 0$ and $0\rightarrow 1$ reaction probabilities.

### C. Microscopic Reversibility and Conservation of Flux

The semiclassical CSC, PSC, and USC transition probabilities all obey microscopic reversibility.[22] The exact quantum ones do also, of course, but the quasiclassical ones do not. We illustrate this property numerically in Table II where the quasiclassical and USC results are given for two energies.

The semiclassical collision probabilities in gen-

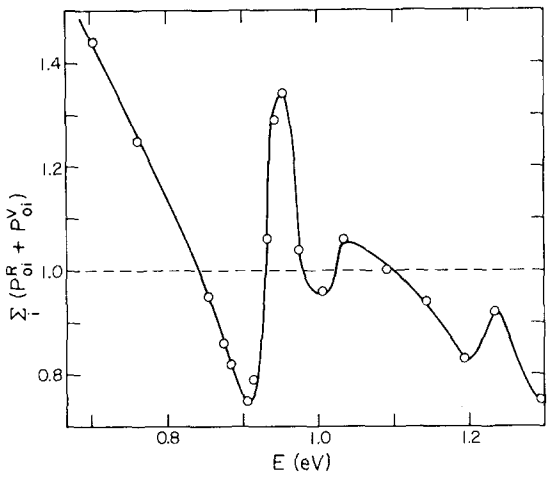


FIG. 11. Total uniform semiclassical collision probabilities as a function of the total energy, $E$.

eral do not sum up to unity and may differ from it by as much as 25%. In Fig. 11 we have plotted the sum of the USC collision probabilities over the total energy range 0.68 eV to 1.28 eV. In some of this energy range this sum is less than unity. This correlates partly with the fact that for certain energies one or more contributing transition probabilities is zero since the corresponding transition is dynamically forbidden. For example, in the energy range 0.85–0.91 eV the reactive and nonreactive $0 \rightarrow 1$ transitions are dynamically forbidden. If the corresponding transition probabilities were calculated by the use of complex trajectories or analytical continuation one might guess that, in analogy with the present reaction threshold behavior, they would increase montonically with increasing energies for energies in the above range. This expectation is consistent with the observed monotonic decrease in the present calculations, since we have not included such methods in the present calculations. For $E$ between 0.91 and 0.953 eV the rapid rise of the USC sum to a maximum of 1.34 is due to the abruptness with which these $0 \rightarrow 1$ transitions become dynamically allowed. The quasiclassical total reaction probabilities are automatically normalized and the quantum results are always within 2% of unity or better.

## IV. DISCUSSION

### A. The Reaction Threshold Region

The threshold behavior of the reactive $0 \rightarrow 0$ transition, important for thermal rate constants, is not described properly by any of the semiclassical expressions used. In Sec. III it was shown that at total energies around 0.55 eV the USC, PSC, and CSC expressions for the $P^R_{00}$ transition probability did not apply. However, a possibly more serious shortcoming of the form of the semiclassical theory used in the present paper is that it furnishes a zero reaction probability at any energy for which no quasiclassical reactive trajectory exists. This is certainly the case in the $H + H_2$ surface here considered for total energies less 0.424 eV—the energy of the saddle point. At these energies the reaction proceeds totally by tunneling. Recently Miller and George[1f,1g] have formulated an approach to this kind of tunneling and applied it to the collinear $H + H_2$ reaction at energies below the classical threshold for the Porter–Karplus surface.[1f,1g] Stine and Marcus[2f] have applied complex-valued trajectories to a model collinear inelastic scattering calculation. These approaches make use of complex-valued trajectories. Freed[23] has shown that tunneling can be described semiclassically by transforming the classical propagator in space–time variables into a space–energy representation involving an integration over time which is allowed to be complex. In our calculations no attempt was made to deal with such nonclassical trajectories. Thus, the USC, PSC, and CSC $P^R_{00}$ probabilities were also set equal to zero for total energies between 0.424 and 0.52 eV. Similarly, the semiclassical $P^V_{00}$ transition probabilities vanish in the total energy range 0.6 to 0.7 eV since no nonreactive quasiclassical trajectories were found in this range.

The extension of semiclassical theory, such as the one made by George and Miller, to include nonclassical trajectories is necessary if the reaction threshold behavior is to be better described. In order to ascertain the accuracy of their approach, we have compared their results for the collinear $H + H_2$ exchange reaction[1g] with the quantum ones for the Porter–Karplus surface. (Whereas all other calculations presented so far were done with Wall–Porter fit to SSMK surface.[12]) In Fig. 12 we have plotted the ratio of the complex-trajectory semiclassical reaction probabilities $P^R_{SC}$ to the accurate quantum ones[11] $P^R_{EQ}$ as a function of translational energy $E_0$. It can be seen that over the energy range of 0.02 to 0.2 eV, of importance for tunneling process, the semiclassical reaction probabilities range from 0.65 to 0.87 of the accurate ones, indicating that for this collinear system the complex-trajectory method used[1g] underestimates the effect of tunneling. The steep rise in the $P^R_{SC}/P^R_{EQ}$ ratio above $E_0 = 0.2$ eV shown in Fig. 12 may be indicative of the same kind of divergent behavior as the one shown in Fig. 3 by the USC $P^R_{00}$ curve.

We have also calculated the collinear rate constants corresponding to the $P^R_{SC}$ and $P^R_{EQ}$ above by a numerical integration of the appropriate expression.[12] The corresponding rate constant ratio $k_{SC}(T)/k_{EQ}(T)$ is plotted in Fig. 13 as a function of

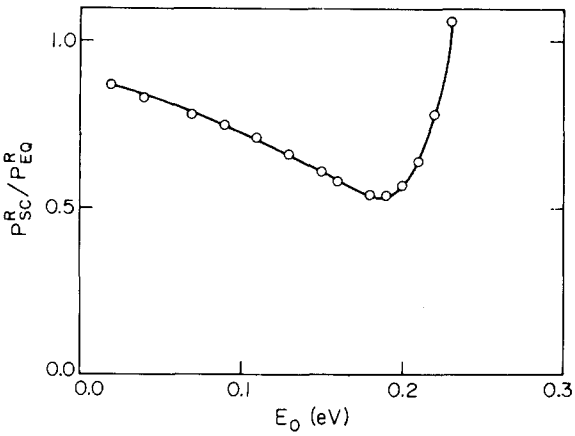


FIG. 12. Ratio of complex-trajectory semiclassical reaction probability $P^R_{SC}$ (taken from Ref. 1g) to exact quantum reaction probability $P^R_{QM}$ (taken from Ref. 11) for very low initial translational energies $E_0$.

$1/T$. It can be seen that in the temperature range from 100 to 300 °K this ratio varies from about 0.65 to about 0.73. This is a significant improvement over the corresponding quasiclassical ratio calculated from the same collinear reaction on a slightly different potential energy surface.[14] The fact that these ratios are less than unity is a manifestation of the fact that this complex-trajectory semiclassical method underestimates tunneling, as just pointed out.

### B. The Reactive and Nonreactive $0 \rightarrow 0$ Transitions Above the Reaction Threshold Region

It has been noted in Sec. III that the reactive $0 \rightarrow 0$ transition becomes dynamically inaccessible at total energies greater than 1.25 eV. In this case, there are no real roots of the equation $m = 0$, and therefore Eqs. (2), (5), and (6) of Sec. 2 are not applicable. Hence the USC, PSC, and CSC $P^R_{00}$ transition probabilities are equal to zero for these energies, as stated in Sec. II and depicted in Figs. 2 and 4. In fact, this result is not a bad approximation to the exact quantum values, which at energies between 1.3 eV and 1.5 eV have an average value of about 0.08. At total energies slightly below 1.25 eV the PSC and CSC $P^R_{00}$ transition probabilities diverge for the reason given in Sec. IV. B, whereas the USC curve shows a behavior quite similar to that of the exact quantum one. This is a manifestation of the improvement obtained in going to the uniform approximation.

The oscillations in the exact quantum curves are not well reproduced by the semiclassical ones especially for the $P^V_{00}$ transition probabilities, as indicated in Figs. 5 and 6. The USC results, however, are in much better average agreement with the exact ones than are the PSC and CSC results. Clearly the attempt by the present semiclassical theory to introduce the quantum effects present in these transitions for this collinear reaction has not succeeded. Apparently such quantum effects are not of a simple interference nature. Indeed, recent lifetime calculations done on the same potential energy surface[24] indicate that the marked quantum oscillations at total energies of 0.90 and 1.28 eV are due to the interference of resonant (compound state) and direct parts of the pertinent S matrix elements. We might say that the present semiclassical theory is aimed at approximating the direct part of the exact S matrix. If this is the case, an illuminating comparison would be one between the present semiclassical transition probabilities and quantum transition probabilities modified so as to exclude (approximately) the effects of the resonant component of the S matrix elements. We expect that the result of such a comparison would show better agreement between the USC and such modified quantum transition probabilities. A composite theory including an approximate treatment of the resonant component and a semiclassical treatment of the direct component of the scattering matrix may be expected to yield a significant improvement.

### C. The Reactive and Nonreactive $0 \rightarrow 1$ Transitions

The USC threshold energies for the $0 \rightarrow 1$ reactive and nonreactive transition probabilities are about 0.08 eV higher than those for the exact quantum

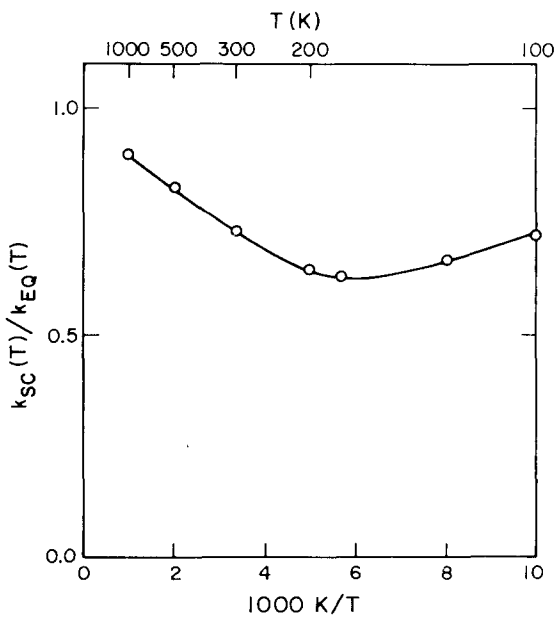


FIG. 13. Ratio of complex-trajectory semiclassical rate constant $k_{SC}(T)$ to exact quantum rate constant $k_{EQ}(T)$ as a function of $1/T$ (lower abscissa) and $T$ (upper abscissa).

calculations but show a similar steep rise as the energy increases above threshold.

The oscillatory behavior of the exact quantum curves is qualitatively displayed by the USC curves especially for the reactive transition, except at $E = 1.28$ eV where a sharp resonance occurs. There is much better overall agreement between the USC and exact quantum results than was the case for the $0 \rightarrow 0$ transition.

Whereas for the $0 \rightarrow 0$ transitions, the quasiclassical results were in better agreement with exact quantum one than the USC results (especially for the reactive case), the reverse is true for the $0 \rightarrow 1$ transitions. This is particularly so in the threshold region, due to the arbitrariness of the quasiclassical definition of the final state quantum number, as mentioned towards the end of Sec. IV. The reverse $P_{10}^R$ quasiclassical results do not suffer from this defect, which partially explains the significant improvement in using this quantity as an approximation to the accurate quantum $P_{01}^R$. However, this does not explain why the $P_{10}^R$ QC results are better than the $P_{01}^R$ ones substantially away from threshold.

## IV. CONCLUSION

The uniform, primitive, and classical semiclassical reactive and non-reactive $0 \rightarrow 0$ and $0 \rightarrow 1$ transition probabilities for the collinear $H + H_2 \rightarrow H_2 + H$ reaction do not in general agree closely with the exact quantum results. As expected, the USC approximation is better than the PSC and CSC ones. The low energy divergent behavior of the reactive and nonreactive $0 \rightarrow 0$ USC, PSC, and CSC transition probabilities is greatly in error. By contrast, the corresponding quasiclassical trajectory results are generally in much better agreement with the exact quantum ones.

Agreement between the USC and exact quantum results for the $0 \rightarrow 1$ transitions is much better than for the $0 \rightarrow 0$ ones. The $0 \rightarrow 1$ USC threshold energies are about 0.08 eV greater than the correct ones, but as the energy increases above the respective thresholds the USC and exact quantum curves show a similar steep rise. In addition there is qualitative agreement between the USC and exact results. The standard quasiclassical results are in poor agreement with the exact ones and as a result the USC results give substantial improvement over the former ones. However, the reverse quasiclassical results also give significant improvement over the usual quasiclassical ones and in fact are not much worse than the USC ones.

A possible explanation for the inability of the semiclassical results reported herein to produce the pronounced quantum effects in this reaction lies in the importance of resonant processes for this reaction. These processes were found to be present in the exact quantum results and the present semiclassical theory does not take such phenomena into account.

*This work was supported in part by the United States Atomic Energy Commission, Report Code No. CALT-767P4-125.

†Work performed in partial fulfillment of the requirements for the Ph.D. degree in Chemistry at the California Institute of Technology.

‡Contribution No. 4744.

[1](a) W. H. Miller, J. Chem. Phys. **53,** 1949 (1970); (b) J. Chem. Phys. **53,** 3578 (1970); (c) W. H. Miller, Chem. Phys. Lett. **7,** 431 (1970); (d) W. H. Miller, J. Chem. Phys. **54,** 5386 (1971); (e) C. C. Rankin and W. H. Miller, J. Chem. Phys. **55,** 3150 (1971); (f) W. H. Miller and T. F. George, J. Chem. Phys. **56,** 5668 (1972); (g) J. Chem. Phys. **57,** 2458 (1972); (h) J. D. Doll, T. F. George, and W. H. Miller, J. Chem. Phys. **58,** 1343 (1973).

[2](a) R. A. Marcus, J. Chem. Phys. **54,** 3965 (1971); (b) J. N. L. Connor and R. A. Marcus, J. Chem. Phys. **55,** 5636 (1971); (c) W. H. Wong and R. A. Marcus, J. Chem. Phys. **55,** 5663 (1971); (d) R. A. Marcus, J. Chem. Phys. **56,** 311 (1972); (e) J. Chem. Phys. **56,** 3548 (1972); (f) J. Stine and R. A. Marcus, Chem. Phys. Lett. **15,** 536 (1972).

[3]R. D. Levine and B. R. Johnson, Chem. Phys. Lett. **7,** 404 (1970).

[4](a) P. Pechukas, Phys. Rev. **181,** 174 (1969); (b) P. Pechukas and J. P. Davis, J. Chem. Phys. **56,** 4970 (1972).

[5]B. C. Eu, J. Chem. Phys. **57,** 2531 (1972).

[6]J. M. Bowman and Aron Kuppermann, Chem. Phys. (to be published).

[7]D. Secrest and B. R. Johnson, J. Chem. Phys. **45,** 4556 (1966).

[8]D. J. Diestler, J. Chem. Phys. **54,** 4547 (1971).

[9]S.-F. Wu and R. D. Levine, Mol. Phys. **22,** 881 (1971).

[10]R. N. Porter and M. Karplus, J. Chem. Phys. **40,** 1105 (1964).

[11]G. C. Schatz and Aron Kuppermann (private communication) have repeated the exact quantum calculations on the Porter–Karplus surface using a fully converged close coupling method and obtained reaction probabilities in agreement with those of Ref. 8. A comparison between these accurate quantum results and the complex-trajectory semiclassical ones is given in Sec. IV.B. of the present paper.

[12]D. G. Truhlar and Aron Kuppermann, J. Chem. Phys. **56,** 2232 (1972).

[13]G. C. Schatz and Aron Kuppermann (to be published).

[14]J. M. Bowman and Aron Kuppermann, Chem. Phys. Lett. **12,** 1 (1972).

[15]F. T. Wall and R. N. Porter, J. Chem. Phys. **36,** 3256 (1962).

[16]I. Shavitt, R. M. Stevens, F. L. Minn, and M. Karplus, J. Chem. Phys. **48,** 2700 (1968).

[17]J. M. Bowman and Aron Kuppermann, Chem. Phys. Lett. **19,** 166 (1973).

[18]H. Goldstein, *Classical Mechanics* (Addison-Wesley, Reading, Mass., 1950) (a) p. 241; (b) Sec. 9-1.

[19]M. Abramowitz and I. Stegun, Eds., *Handbook of Mathematical Functions* (U. S. Govt. Printing Office, Washington, D.C., 1964), pp. 446–452.

[20]B. Carnahan, H. A. Luther, and J. O. Wilkes, *Applied Numerical Methods* (Wiley, New York, 1969), pp. 361, 386.

[21]In Ref. 14 the phrase "we assign to this diatom the quantum number $v = n$ if $E(n) \leq E_{Cl}^{v} < (1/2)\Delta E(n)$" should have

read "we assign to this diatom the quantum number $v = n$ if $E(n) \leq E^{v}_{\mathrm{Cl}} < E(n) + (1/2)\Delta E(n)$."

[22]To show that the semiclassical expressions obey microscopic reversibility it suffices to demonstrate that $\Delta_2 - \Delta_1 = \Delta_1 - \Delta_2$ and that $|\partial m^{\beta}/\partial q_0^{\alpha}|^{-1} = |\partial n^{\alpha}/\partial q_1^{\beta}|^{-1}$ (see Eqs. 2, 5, 6, and 7). From Eq. 4 it is clear that upon time-reversal $\Delta_j \rightarrow -\Delta_j$ and hence $\Delta_2 - \Delta_1 = \Delta_1 - \Delta_2$. It has been shown previously[1a] that the Jacobian factor $|\partial m^{\beta}/\partial q_0^{\alpha}|^{-1}$ is equal to $|\partial^2 \phi(m^{\beta}, n^{\alpha})/\partial m^{\beta} \partial n^{\alpha}|$. The phase function $\phi(m^{\beta}, n^{\alpha})$ can be differentiated with respect to $n^{\alpha}$ or $m^{\beta}$ in either order. This fact coupled with the properties that $|\partial \phi(m^{\beta}, n^{\alpha})/\partial n^{\alpha}| = q_0^{\alpha}$ and $|\partial \phi(m^{\beta}, n^{\alpha})/\partial m^{\beta}| = q_1^{\beta}$ gives the desired equality between $|\partial m^{\beta}/\partial q_0^{\alpha}|^{-1}$ and $|\partial n^{\alpha}/\partial q_1^{\beta}|^{-1}$.

[23]K. F. Freed, J. Chem. Phys. **56,** 692 (1972).

[24]G. C. Schatz and Aron Kuppermann, J. Chem. Phys. 59, 964 (1973).